Available Online at http://www.journalajst.com

ASIAN JOURNAL OF SCIENCE AND TECHNOLOGY

ISSN: 0976-3376

Asian Journal of Science and Technology
Vol. 10, Issue, 02, pp.9431-9448, February, 2019

RESEARCH ARTICLE

MIXED CONVECTIVE PASSIVE VENTING IN THE BUILDING WITH DIFFERENT INLET AND EXIT OPENINGS LOCATION ON THE HEATED AND COLD VERTICAL SIDE WALLS CONFIGURATIONS

***Yawovi Nougbléga, Kodjo Kpode and Kokou N'wuitcha**

Laboratoire Sur l'Energie Solaire /Groupe Phénomène de Transfert et Energétique - Université de Lome, Togo

ARTICLE INFO

Article History:

Received 08th November, 2018
Received in revised form
15th December, 2018
Accepted 12th January, 2019
Published online 28th February, 2019

Key words:

Mixed convection, Numerical study, Passive venting, Thermal comfort, Heat transfer.

****Corresponding author:***
Yawovi Nougbléga,

ABSTRACT

A numerical study is conducted to investigate mixed convective venting of a two-dimensional rectangular cavity with different located inlet and outlet openings on the heated and the cold side walls. The horizontal walls are assumed to be adiabatic. Fresh air is blown into the cavity from the different located inlets in the side walls of the cavity and is exited through the different outlets located in the vertical side walls. These configurations of mixed convective heat transfer have application in building saving energy systems, cooling of electronic circuit boards, and solar collectors, among others. The aim of this research is to optimize the relative locations of inlet and outlet in order to have most effective cooling in the core of the cavity by maximizing the heat-removal rate and reducing the overall temperature in the cavity. Three placement configurations of the inlets and outlets are examined for a range of Reynolds and Grashof numbers. For a given Reynolds number, the Grashof number is varied from 0, which represents pure forced convection, to 106, which implies a dominant buoyancy effect. Injection of the fresh air at the top and bottom of the heated and cold walls is studied and the results are presented in the form of isotherms, streamlines, velocity and local Nusselt number at the left heated wall. It is observed that maximum cooling effectiveness is achieved if the injections from the bottom and the top of the heated wall and exits from the bottom and the top of the cold wall where forced and natural convection aid each other.

Citation: Yawovi Nougbléga, Kodjo Kpode and Kokou N'wuitcha, 2019. "Mixed convective passive venting in the building with different inlet and exit openings location on the heated and cold vertical side walls configurations", *Asian Journal of Science and Technology*, 10, (02), 9431-9448.

INTRODUCTION

Mixed convection flows in rectangular cavities are encountered in a wide variety of heat transfer equipment and environmental situations. Hence, a number of studies concerning the mixed convection phenomenon in cavities have been reported in order to investigate the heat transfer and fluid flow in such geometries. This obvious interest is dictated by a direct relationship between the air refreshment and the convection phenomenon. The existing literature in this domain has focused considerable attention on mixed convection in cavities, and especially on the limit of predominance of forced convection. In fact, (Simoneau *et al.,* 1989) have shown that the maximum and minimum contributions of mixed convection in the heat evacuation are obtained for $Re^2/Gr = 2 X10^{-3}$ and $Re^2/Gr = 3 x10^{-3}$ respectively. Results of the study of (Safi and Loc, 1994) obtained in the case of a ventilated square cavity, show that a thermal stratification appears for $Gr/Re^2 = 1$ when the horizontal walls of the cavity were considered adiabatic. The relative importance of natural convection compared to forced convection was examined analytically by (Yao, 1983). The presented solutions indicate that the natural convection becomes the dominant heat transfer mode when $Gr > Re$ in the case of constant wall temperature, and $Gr^2 > Re$ in the case of constant wall heat flux. The numerical calculations of (Humphrey and To, 1986), relative to a differentially heated cavity with one hydrodynamically driven wall, reveal that the Nusselt number is minimum for $Re^2/Gr \backsimeq 1$ and the flow becomes independent of the inclination of the cavity when the parameter Re^2/Gr is greater than 21.3. (Hsu *et al.,* 1997) have studied numerically the mixed convection in a square enclosure with a partially dividing partition. Their results show that the average Nusselt number increases by increasing Re at a given value of Gr/Re^2 and also by increasing Gr/Re^2 for a constant value of Re. Quantitative results of the simulations indicate that the heat dissipated from the source is maximum when the outflow opening is placed at the lower part of the vertical wall. A better heat removal was also obtained when the heat source was placed as close as possible to the cold stream inlet opening. In a recent numerical study, (Raji and Hasnaoui,1998a) obtained results for opposing flows (forced and natural flows) in a rectangular cavity heated from the side with a constant heat flux and submitted to a laminar cold jet from the bottom of its heated wall. The fluid leaves the cavity via the top (BT configuration) or the bottom (BB configuration) of the opposite vertical wall. The maximum Nusselt number was obtained for critical values of Re correlated by $Rem = 9.982\ Ra^{0.175}$ and $Rem = 1.3833\ Ra^{0.3618}$ respectively for the BT and BB configurations. Hence the

effectiveness of such a heating system depends on various factors including the duct geometry, location, and orientation of supply air outlets, return air inlets, outlet velocity, and the room configuration. For the purpose of designing the heating and ventilation system, detailed knowledge of the velocity and temperature profiles in the room are helpful. With the continuous improvements in the field of Computational Fluid Dynamics(CFD). Elsewhere, the flow is more likely to be laminar or weakly turbulent and unsteady. In the context of heating or cooling in warm climates, these flows are buoyant, and in some cases, buoyancy drives the mean flow motion. The presence of walls creates the so-called near wall regions, where the turbulent transport is significantly influenced by a solid surface. In practical applications, the obstructions within the room create geometrical complexity. In reality, most air flows are inherently three-dimensional and unsteady. Shear layers, on the periphery of supply air jet and recirculation within the room, add to the complexity of the flow. Due to these characteristics, airflows in room present a great challenge for the available numerical models. Nowadays, very effective insulation materials are being used in air-conditioned buildings, which have considerably reduced the heating/cooling loads, and thereby, the air supply rates have also considerably reduced. Hence, laminar and low Reynolds number turbulent flow modeling studied by (Jones and Lounder, 1972) is gaining increasing importance for room air flows (Terai, 1959) made the first attempt at the numerical calculation of indoor airflow for the case of two-dimensional buoyant flow. Since then, many researchers have made extensive efforts to develop a numerical prediction method, which could be used as a practical tool for indoor environmental design. Nomura and (Kaizuka, 1973), (Tsuchiya, 1973) and (Yamazaki *et al.,* 1976) made the first few practical and important contributions independently for the two-dimensional laminar flows. These research efforts were followed by (Nomura *et al.,* 1975) for three-dimensional laminar flows using the Marker and Cell method. They also made qualitative comparisons of their results with flow visualization experiments. Natural convection in enclosures has been a topic of great interest. (Catton, 1979) and (Ostrach, 1972) reviewed the literature pertaining to natural convection in enclosures.

The study of the transient removal of a contaminant from two-dimensional enclosure has been carried out by (Lage *et al.,* 1991, 1992). It has been shown that significant gains in ventilation efficiency can be made by properly orienting and positioning the inlet and outlet ports relative to each other and to the enclosure. Extensive research has been carried out by numerous authors on CFD in room for various types of inlets, outlets, and flow conditions, as reported in review articles by (Kato *et al.,* 1994) and (Murakami *et al.,* 1993). Natural convection in partitioned enclosures has been reported by many authors and it has been reviewed in a recent paper by (Hsu *et al.,* 1997). Then (Lee *et al.,* 1997) applied finite element method to study the characteristics of forced and mixed convection in an air-cooled room for both laminar and turbulent regimes. Most of the previous studies on heating and ventilation in rooms have been dealt with a limited range of Gr/Re^2 signifying ratio of buoyancy to inertia effects. for some fixed locations of inlet and outlet. This investigation considers air flow and heat transfer in a room for various locations of inlet and outlet at high values of Gr/Re^2. The velocity and temperature distributions in a room have been found by solving Navier Stokes and energy equations, numerically by finite volume method employing Semi Implicit Method for Pressure Linked Equation-Consistent (SIMPLEC) algorithm. Laminar mixed convection in enclosures as investigated here also finds application in modeling solar collectors (Shaw *et al.,* 1993) and cooling of electronic chips (Williams *et al.,* 1994) and (Baek *et al.,* 1997). The aim of the present investigation is to contribute to the enrichment of the knowledge acquired in passive venting in the enclosures by considering the effect of the inlets and outlets openings locations in the heated cavities .This effect will be examined for three configurations realizing lower mean temperatures in the cases.

Problem formulation

The three different configurations of two-dimensional room model under study with the system of coordinates are sketched in Fig. 1. It consists that the ventilated building heated by a uniform heat flux from its vertical left wall while the remaining walls are considered perfectly insulated. The system is submitted to an imposed flow of fresh air, parallel to the horizontal walls, entering the building from one or two inlet openings located respectively at the bottom or the top of the left or the right vertical wall for the room and leaving through the outlet openings. The third dimension of the building (direction perpendicular to plane of the diagram) is assumed to be large enough so that the fluid motion can be considered two-dimensional. The flow is assumed to be laminar and incompressible with negligible viscous dissipation. All the thermophysical properties of the coolant fluid are assumed constant except the density gives rise to the buoyancy forces (Boussinesq approximation). Taking into account the above-mentioned assumptions, the non-dimensional governing equations, written in vorticity – streamlines ($\boldsymbol{\omega}$-ψ) formulation, are as follows:

Mathematical formulation

Governing equations

$$\frac{\partial U}{\partial X}+\frac{\partial V}{\partial Y}=0 \qquad \text{..... (1)}$$

$$\frac{\partial \omega}{\partial \tau}+U\frac{\partial \omega}{\partial X}+V\frac{\partial \omega}{\partial Y}=Ri\frac{\partial \theta}{\partial X}+\frac{1}{Re}\left(\frac{\partial^2 \omega}{\partial X^2}+\frac{\partial^2 \omega}{\partial Y^2}\right) \qquad \text{..... (2)}$$

$$\frac{\partial \theta}{\partial \tau}+U\frac{\partial \theta}{\partial X}+V\frac{\partial \theta}{\partial Y}=\frac{1}{RePr}\left(\frac{\partial^2 \theta}{\partial X^2}+\frac{\partial^2 \theta}{\partial Y^2}\right) \qquad \text{..... (3)}$$

$$\omega=-\left(\frac{\partial^2 \Psi}{\partial X^2}+\frac{\partial^2 \Psi}{\partial Y^2}\right) \qquad \text{..... (4)}$$

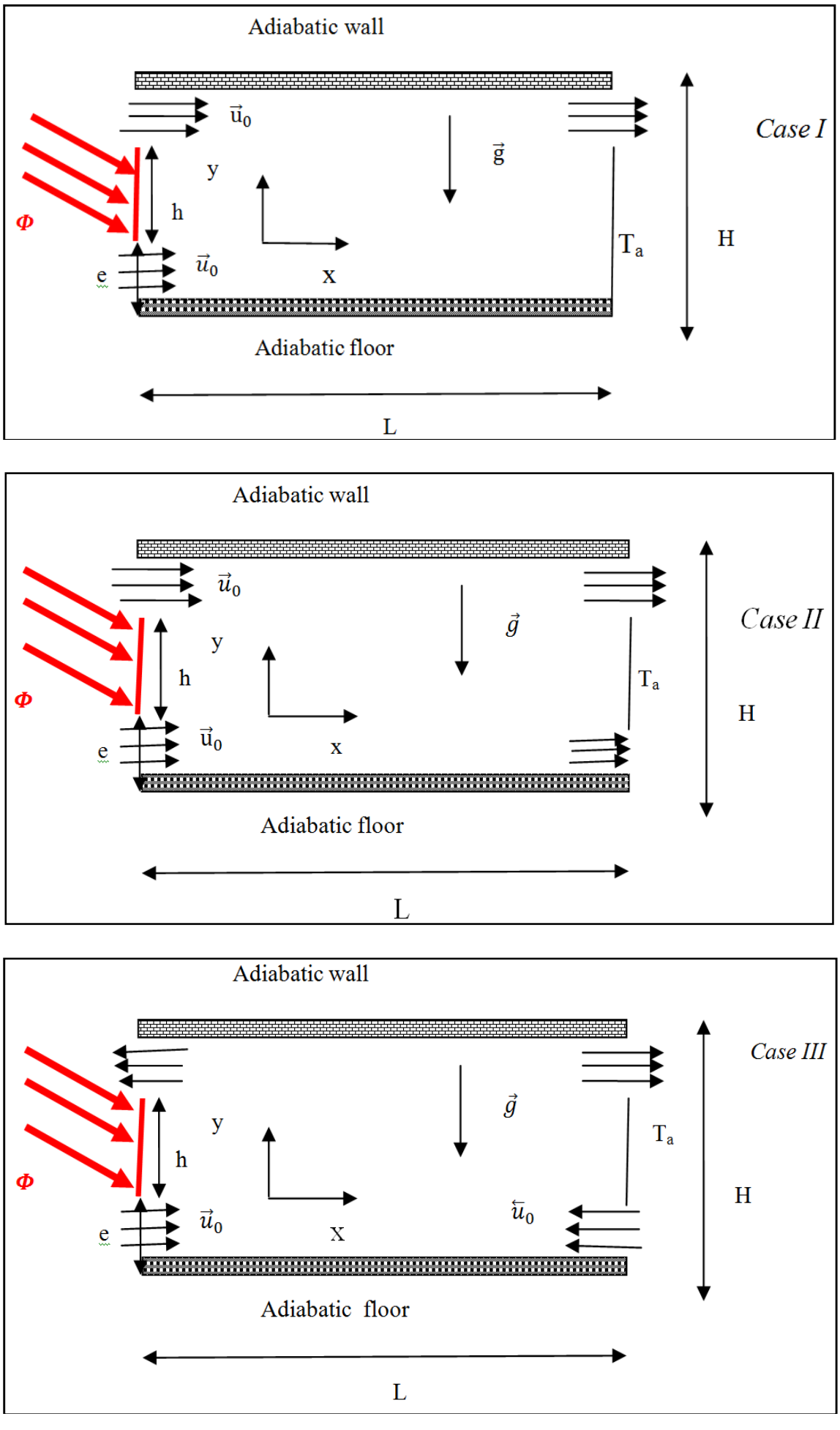

Fig.1. Schematic of inlets and outlets openings locations in the room

Boundary Conditions

- Initial conditions: at $\tau = 0$:

$$\theta = \omega = U = V = \psi = 0 \quad \text{..... (5)}$$

- at $\tau > 0$

The boundary conditions associated with the problem are found below.

At the left, right, top and bottom walls: No slip and impermeability boundary conditions have been used on all walls except at inlets and outlets openings.

Configuration Case I

$$X = 0 \; and \; 0 < Y < E; U = 1, \psi = Y, V = \omega = \theta = 0$$

$$X = 0 \; and \; E < Y < B; U = V = \psi = 0, \omega = -\frac{\partial^2 \psi}{\partial x^2}\Big|_{X=0}, \frac{\partial \theta}{\partial X}\Big|_{X=0} = -1 \quad \text{..... (6)}$$

$$X = 0 \; and \; D < Y < 1; U = 1, \psi = Y - D, V = \omega = \theta = 0$$

$$X = A \; and \; 0 < Y < D; U = V = \psi = 0, \omega - \frac{\partial^2 \psi}{\partial X^2}\Big|_{X=A}, \theta = 0$$

$$X = A \; and \; D < Y < 1; \frac{\partial \theta}{\partial Y}\Big|_{X=A} = \frac{\partial \psi}{\partial Y}\Big|_{X=A} = \frac{\partial \omega}{\partial Y}\Big|_{X=A} = \frac{\partial U}{\partial Y}\Big|_{X=A} = \frac{\partial V}{\partial Y}\Big|_{X=A} = 0$$

$$Y = 0 \; and \; 0 < X < A; U = V = \psi = 0, \omega = -\frac{\partial^2 \psi}{\partial Y^2}\Big|_{Y=0}, \frac{\partial \theta}{\partial Y}\Big|_{Y=0} = 0$$

$$Y = 1 \; and \; 0 < X < A; U = V = \psi = 0, \omega = -\frac{\partial^2 \psi}{\partial Y^2}\Big|_{Y=1}, \frac{\partial \theta}{\partial Y}\Big|_{Y=1} = 0$$

Configuration Case II

$$X = 0 \; and \; 0 < Y < E; U = 1, \psi = Y, V = \omega = \theta = 0$$

$$X = 0 \; and \; E < Y < B; U = V = \psi = 0, \omega = -\frac{\partial^2 \psi}{\partial x^2}\Big|_{X=0}, \frac{\partial \theta}{\partial X}\Big|_{X=0} = -1$$

$$X = 0 \; and \; D < Y < 1; U = 1, \psi = Y - D, V = \omega = \theta = 0$$

$$X = A \; and \; 0 < Y < E; \frac{\partial \theta}{\partial Y}\Big|_{X=A} = \frac{\partial \psi}{\partial Y}\Big|_{X=A} = \frac{\partial \omega}{\partial Y}\Big|_{X=A} = \frac{\partial U}{\partial Y}\Big|_{X=A} = \frac{\partial V}{\partial Y}\Big|_{X=A} = 0$$

$$X = A \; and \; E < Y < B; U = V = \psi = 0, \omega = -\frac{\partial^2 \psi}{\partial x^2}\Big|_{X=A}, \theta = 0$$

$$X = A \; and \; D < Y < 1; \frac{\partial \theta}{\partial Y}\Big|_{X=A} = \frac{\partial \psi}{\partial Y}\Big|_{X=A} = \frac{\partial \omega}{\partial Y}\Big|_{X=A} = \frac{\partial U}{\partial Y}\Big|_{X=A} = \frac{\partial V}{\partial Y}\Big|_{X=A} = 0$$

$$Y = 0 \; and \; 0 < X < A; U = V = \psi = 0, \omega = -\frac{\partial^2 \psi}{\partial Y^2}\Big|_{Y=0}, \frac{\partial \theta}{\partial Y}\Big|_{Y=0} = 0$$

$$Y = 1 \; and \; 0 < X < A; U = V = \psi = 0, \omega = -\frac{\partial^2 \psi}{\partial Y^2}\Big|_{Y=1}, \frac{\partial \theta}{\partial Y}\Big|_{Y=1} = 0$$

Configuration Case III

$$X = 0 \; and \; 0 < Y < E; U = 1, \psi = Y, V = \omega = \theta = 0$$

$$X = 0 \; and \; E < Y < B; U = V = \psi = 0, \omega = -\frac{\partial^2 \psi}{\partial x^2}\Big|_{X=0}, \frac{\partial \theta}{\partial X}\Big|_{X=0} = -1$$

$X = 0\ and\ D < Y < 1; \left.\frac{\partial\theta}{\partial Y}\right|_{X=0} = \left.\frac{\partial\psi}{\partial Y}\right|_{X=0} = \left.\frac{\partial\omega}{\partial Y}\right|_{X=0} = \left.\frac{\partial U}{\partial Y}\right|_{X=0} = \left.\frac{\partial V}{\partial Y}\right|_{X=0} = 0$

$X = A\ and\ 0 < Y < E; U = -1, \psi = -Y, V = \omega = \theta = 0$

$X = A\ and\ E < Y < B; U = V = \psi = 0, \omega = -\left.\frac{\partial^2\psi}{\partial x^2}\right|_{X=A}, \theta = 0$

$X = A\ and\ D < Y < 1; \left.\frac{\partial\theta}{\partial Y}\right|_{X=A} = \left.\frac{\partial\psi}{\partial Y}\right|_{X=A} = \left.\frac{\partial\omega}{\partial Y}\right|_{X=A} = \left.\frac{\partial U}{\partial Y}\right|_{X=A} = \left.\frac{\partial V}{\partial Y}\right|_{X=A} = 0$

$Y = 0\ and\ 0 < X < A; U = V = \psi = 0, \omega = -\left.\frac{\partial^2\psi}{\partial Y^2}\right|_{Y=0}, \left.\frac{\partial\theta}{\partial Y}\right|_{Y=0} = 0$

$Y = 1\ and\ 0 < X < A; U = V = \psi = 0, \omega = -\left.\frac{\partial^2\psi}{\partial Y^2}\right|_{Y=1}, \left.\frac{\partial\theta}{\partial Y}\right|_{Y=1} = 0$

The stream function and the vorticity are related to the velocity components by the following expressions:

$U = \frac{\partial\psi}{\partial Y}$, $V = -\frac{\partial\psi}{\partial X}$ and $\omega = \left(\frac{\partial V}{\partial X} - \frac{\partial U}{\partial Y}\right)$

Where the scales are defined: $(X, Y) = \left(\frac{x}{H}, \frac{y}{H}\right)$;$\tau = \frac{u_0 t}{H}$;$(U, V) = \left(\frac{u}{u_0}, \frac{v}{u_0}\right)$

$\Psi = \frac{\psi}{u_0 H}$; $\omega = \frac{\Omega\, H}{u_0}$; $\theta = \frac{\lambda(T - T_a)}{\emptyset H}$; $Re = \frac{\rho u_0 (2e)}{\mu}$; $Gr = \frac{\rho^2 g\, \beta\, \emptyset\, (H)^4}{\lambda\, \mu^2}$ ..... (7)

and the aspect ratio expressed as : $A = L/H$; $E = e/H$: $B = h/H$, $D = (h + e)/H$

Evaluation of the model characteristic

From the engineering viewpoint, the most important concern is the heat transfer through the heated walls. These are best represented by Nusselt number, which is a measure of the ratio of the heat transfer by conduction to the flux convected by fluid flow. The local Nusselt number on the heated walls are given by:

$Nu_w = \frac{\emptyset\, H}{\lambda(T_W - T_a)} = 1/\theta_w$ ..... (8)

Method of solution

The non linear partial differential governing equations, (1-3), were discretized using a finite difference technique. The first and second derivatives of the diffusive terms were approached by central differences while a second order upwind scheme was used for the convective terms to avoid possible instabilities frequently encountered in mixed convection problems. The integration of equations (2-3) was assured by Thomas algorithm. At each time step, the Poisson equation, Eq. (4), was treated by using the Point Successive Under-Relaxation method (PSUR) with an optimum under-relaxation coefficient equal to 0.8 for the non uniform grid (121×61) adopted in the present study. Convergence of iteration for stream function solution is obtained at each time step .The following criterion is employed to check for steady-state solution. Convergence of solutions is assumed when the relative error for each variable between consecutive iterations is recorded below the convergence criterion ε such that $\sum\left|\left(\emptyset_{i,j}^{n+1} - \emptyset_{i,j}^{n}\right)/\emptyset_{i,j}^{n+1}\right| < 10^{-5}$ where ϕ stands for ψ, Θ, ω, n refers to time and i and j refer to space coordinates. The time step used in the computations is 10^{-5}. Grid independency solutions are assured by comparing different grid meshes for the highest Grashof and Reynolds numbers used in this work (Gr =10^6 and Re = 200).

The vorticity computational formula of (Woods, 1954) for approximating the wall vorticity was used:$\omega_P = \frac{1}{2}\omega_{P+1} - \frac{3}{\Delta\eta^2}(\psi_{P+1} - \psi_P)$,where ψ_P and ψ_{P+1} are stream function values at the points adjacent to the boundary wall; n the normal abscise on the boundary wall.

Table 1. Grid independency

Grid size	Ψ_{max}	Change(%)	Θ_{max}	Change(%)	Nu_{moy}	Change(%)
61X31	0.23333	-	0.21806	-	8,36906	-
81X41	0.24827	6.01764	0.21081	3.43911	8,90097	5.97586
101X51	0.23892	3.91344	0.20804	1.33147	9,26261	3.90429
121X61	0.24920	0.41252	0.20742	0.29891	9,45675	2.05292

Validation

In order to test the computer code developed for this study, the problem of a ventilated rectangular enclosure with its left and upper walls submitted to a constant heat flux, while the remaining walls are considered adiabatic was studied. Very good agreement is obtained between the test problem solution and the ventilated rectangular enclosure solutions according to (A. Raji *et al.,* 2000) work.

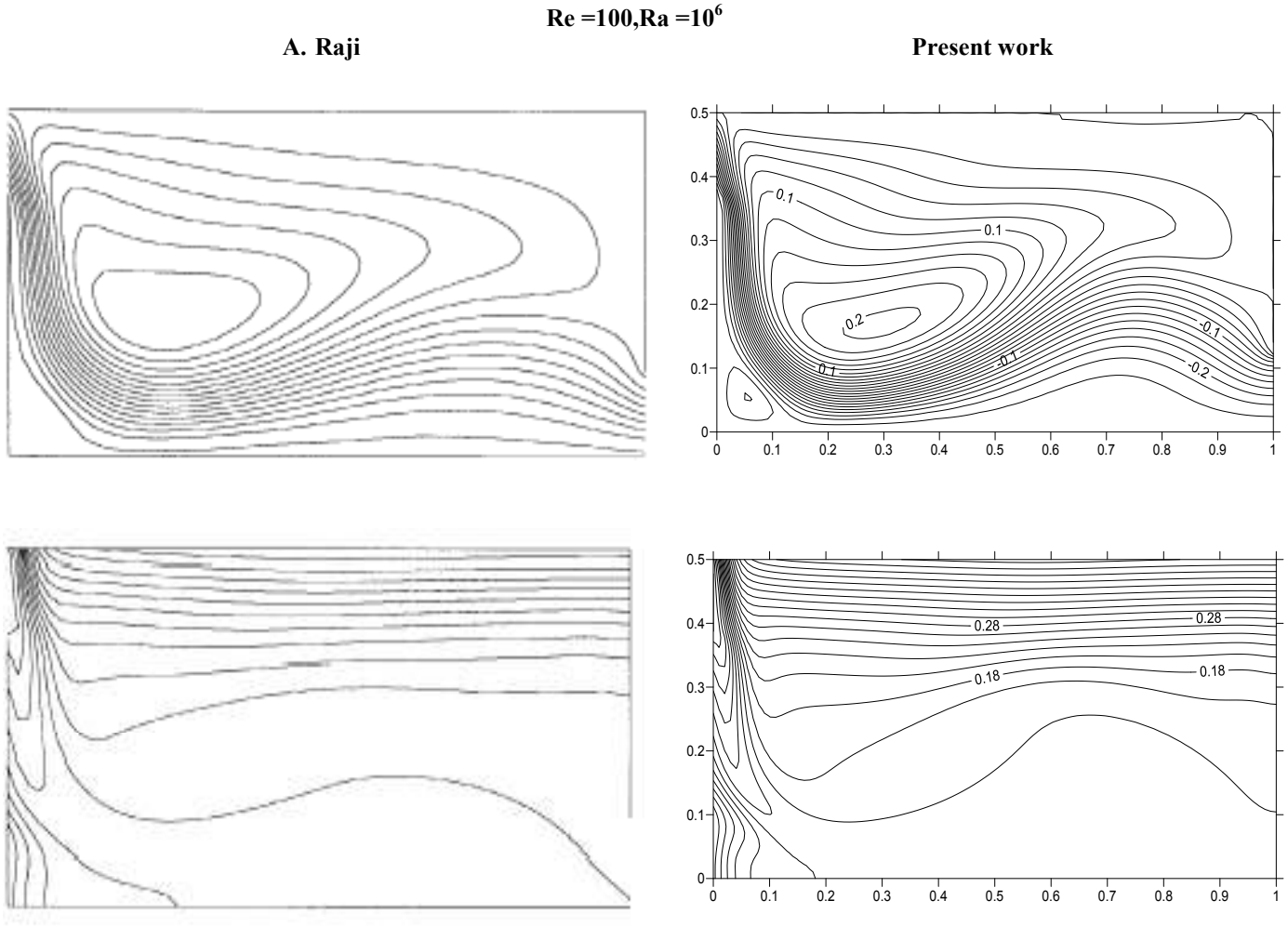

Fig.2.Comparison of streamlines and isotherms

Where the horizontal cold jet enters into the enclosure from the top of its heated wall and leaves from the bottom of the other vertical one with no slip boundary conditions applied to all the walls. The Reynolds number, Re was set at100, for Raleigh number Ra set at10^6 .The numerical analysis predicted values of streamlines and isotherms together with ventilated rectangular enclosure results are shown in Fig.2.

RESULTS AND DISCUSSION

Configuration Case I**:** *Injections at the bottom and the top of the heated wall and exit from the top of the cold wall where forced and natural convection aid each other*

Dynamic and Thermal Field

Influence of grashof number

Fig.3(a-d) shows the dynamic and thermal field for configuration case I (injections at the bottom and the top of the hot wall and exit from the top of the cold wall) in terms of the streamlines and isotherms. The streamlines describe the interaction of forced and natural convection under various grashof number at fixed Reynolds number (Re =10). For Ri = 0, forced convection dominates and major flow is diagonal from the inlet at the bottom of the heated wall to the exit. At higher Gr (10^4 < Gr < 10^6), large recirculation zones are formed above the main fluid stream. There is a hardly distortion of the open lines in the flow streams when the Grashof number is increasing. The natural closed cells near the left heated wall disappear progressively in favour for the distorted open lines.

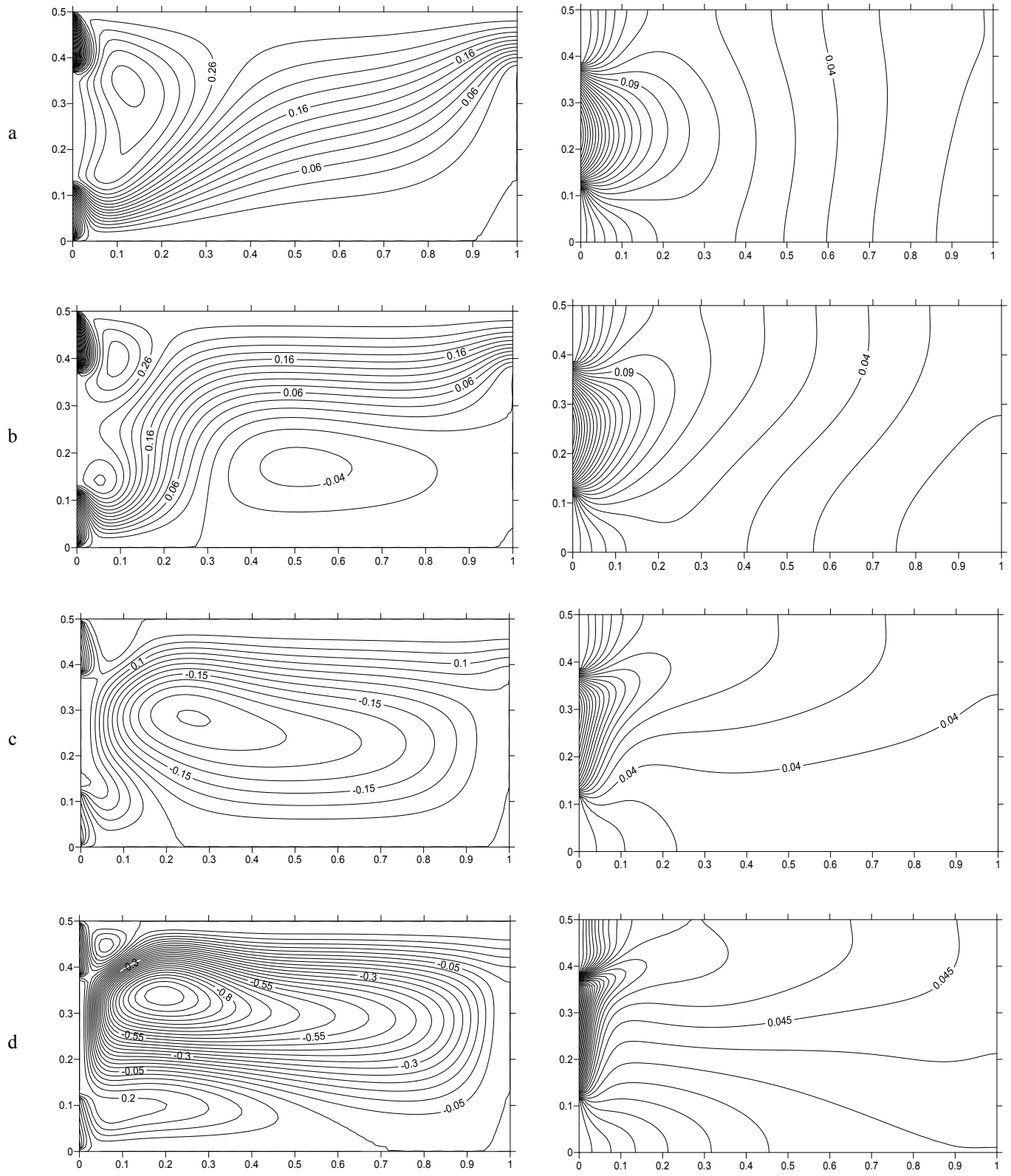

Fig.3. Streamlines and isotherms obtained for Re =10 and various values of Gr : (a) Gr =0 ; (b) Gr =10^4; (c) Gr = 10^5; (d) Gr =10^6

This behavior situation indicates that the mixed convection manifestation in the vented cavity. The buoyancy effects dominate and the main fluid stream rises vertically along the hot wall and travels along the top wall until it exits the cavity at lower Gr (10^4), whereas at higher Gr (10^5 and 10^6) the flow bifurcates with one stream flowing along the hot and top walls and the other flowing in the vicinity of the bottom and cold wall. Thermal field is governed more or less by interaction between incoming fresh air stream and the circulating vortex. For increasing Grashof number or the heat flux intensity, the high-temperature region is more concentrated near the left heated wall and the temperature distribution is more uniform in the remaining parts of the cavity. On the other hand, large temperature gradients close to the hot wall and stratified temperature distribution in the rest of the cavity are observed for any value of Gr.

Influence of Reynolds number

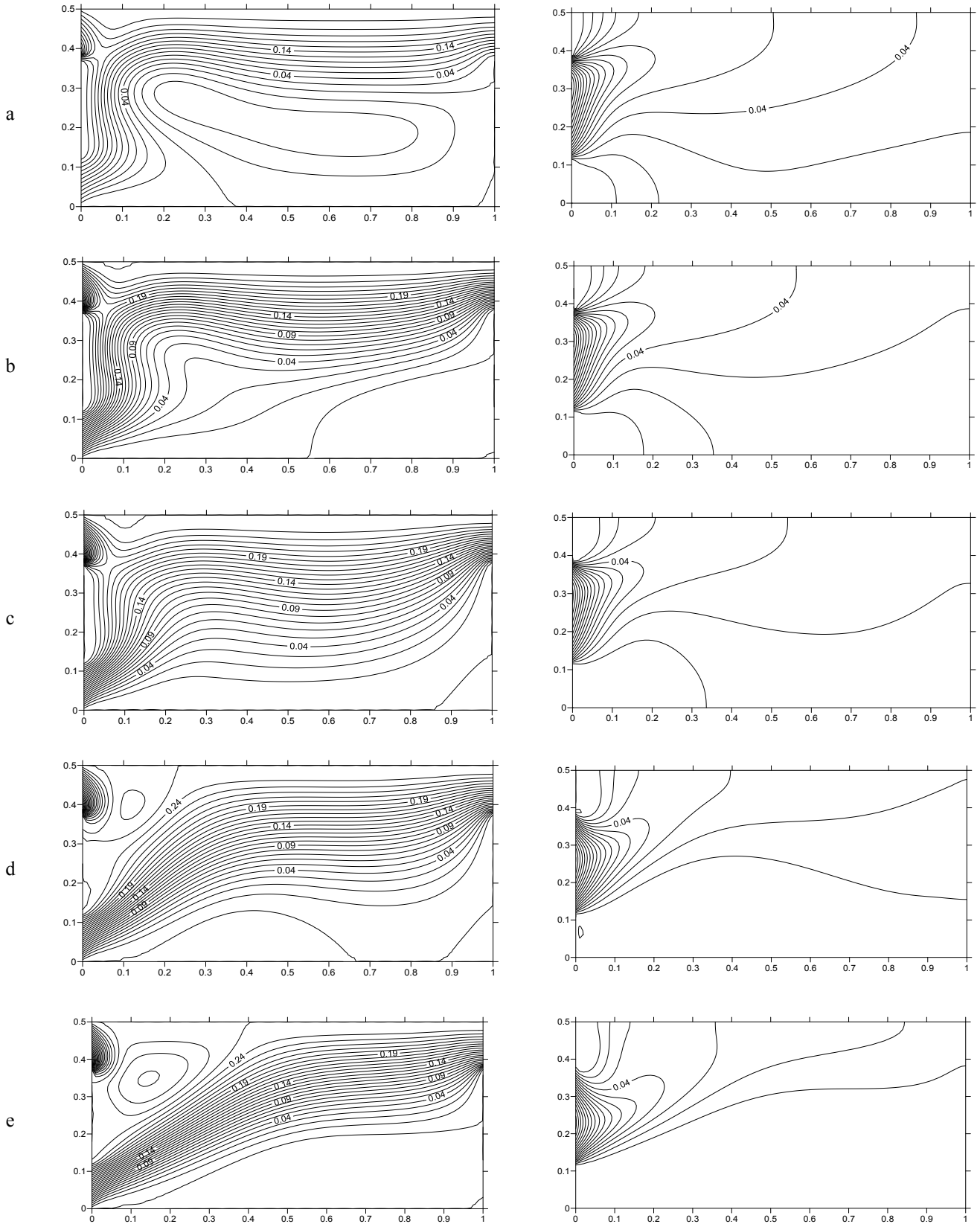

Fig.4. Streamlines and isotherms obtained for Gr=10^5 and different values of Re: (a) Re=20; (b) Re=30; (c) Re= 50; (d) Re= 100; (e) Re=150

The effect of the Reynolds number on the flow structure and temperature distribution is shown in Fig.4(a – e). The streamlines and the isotherms are presented for steady state flows obtained for Gr = 10^5 and values of the Reynolds number ranging between 20 and 150. For Re = 20, the analysis of the streamlines in Fig. (4a) reveals a complex structure in the whole cavity where the presence of the closed cells and open lines is observed.

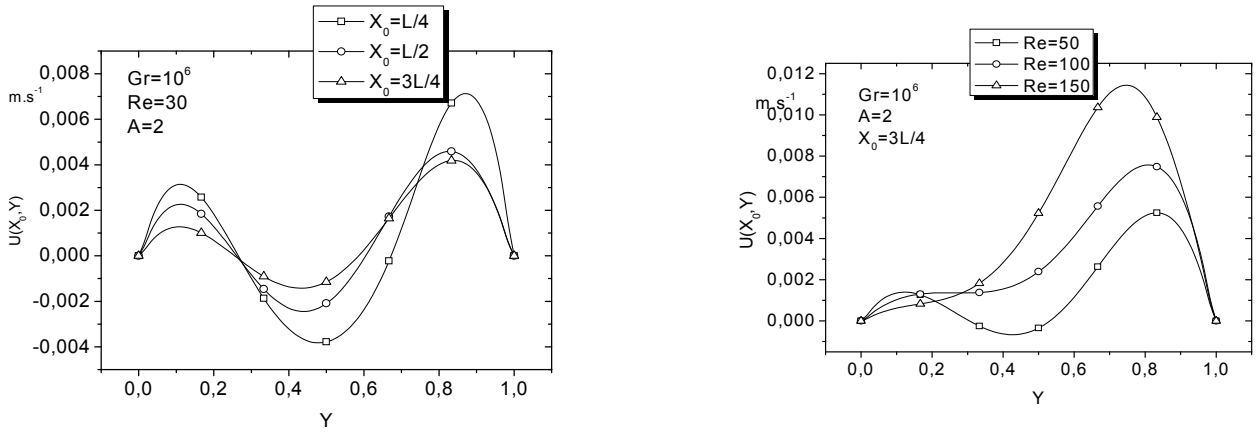

(a) Horizontal component

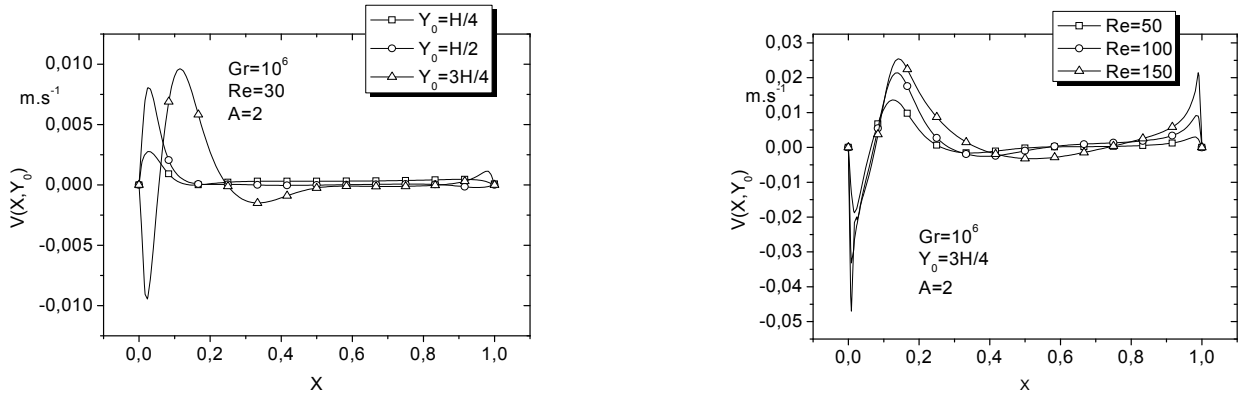

(b) Vertical component

Fig. 5.Variation of the velocity components for various Reynolds numbers

The lower closed cells is located just in front of the lower entry opening, above the open lines, and its presence is imposed by the forced flow. In fact, the heated portion of the left wall, located above the entry openings, imposes a clockwise circulation, but at low Re where the natural convection effect is important. The distribution of the temperature field shows that the lower part of the cavity (far from the heated wall) is at the temperature of the external flow. The lower closed cells will play an increasingly important role by increasing Re since more intense is the forced flow, more important is its negative (positive) effect on the natural convection flow in the upper (lower) part of the cavity. This tendency is already visible in Fig. (4b) for Re = 30. In fact, it is clearly visible from Fig. (4b) that this relatively limited increase of Re is accompanied by a reduction of the size and the intensity of the lower closed cells in favor of the open lines and the tendency is supported by the increase of Re until the total disappearance of the lower closed cells. Indeed, the role played by natural convection is weakened (supported) in the upper (lower) part of the cavity by increasing Re. When the forced flow overcomes the effect of natural convection in the upper part of the cavity, the open lines are aspired by the heated surface above the aperture as indicated in Fig. (4c) for Re = 50. The corresponding isotherms are more tightened at the vicinity of the left heated wall testifying of a noticeable increase in convective heat exchange. In addition, a net progression of the cold zone towards the right cold wall is observed. A further increase of the Reynolds number acts in increasing the aiding role of forced and natural convection in the lower part of the cavity. Hence, the intensification of the forced flow leads to an increase of the role played by the upper closed cells as shown in Fig. 4(d–e), respectively, for Re = 100 (Ri = 10) and Re = 150 (Ri = 4.44). It can also be seen that the forced flow crosses directly the cavity from the two entry openings to the outlet opening without being constrained to go along the left heated wall before reaching the exit, which favors the formation of the recirculation cells of different sizes in the upper part of the cavity. The analysis of the isotherms shows that except the zone near the heated left wall, the remain part of the cavity is maintained isothermal and cold due to the absence of thermal interaction between the forced flow and the heated boundaries. Fig.6 (a-b) showed the variation of the velocity components along the horizontal and the vertical axis. The velocity components are increasing function of Reynolds number. The maximum values of the velocity components observed near the left heated wall indicated that the heat and mass transfers are very important along this one. Hence the negative values indicated the recirculation zones in the vented cavity. The fig.6(a-d) indicates that the maximal value of the temperature is observed near the left heated wall. One can observe in fig.6(c) that the temperature decreases when the Reynolds number is increasing while it increases by increasing the Grashof number, fig.6(d). This obvious situation is explained that since the intensity of the inlet jet of the fresh air is important, greater is the heat transfer exchange in the vented cavity. Then the thermal comfort is obtained by increasing the inlet jet fresh air intensity. Fig.6(a, b) showed that the temperature is stratified along the horizontal as the vertical axis. In fig.7(a,b), the local Nusselt number decreases in the first time before increases in the second time along the heated wall for various grashof or Reynolds numbers.

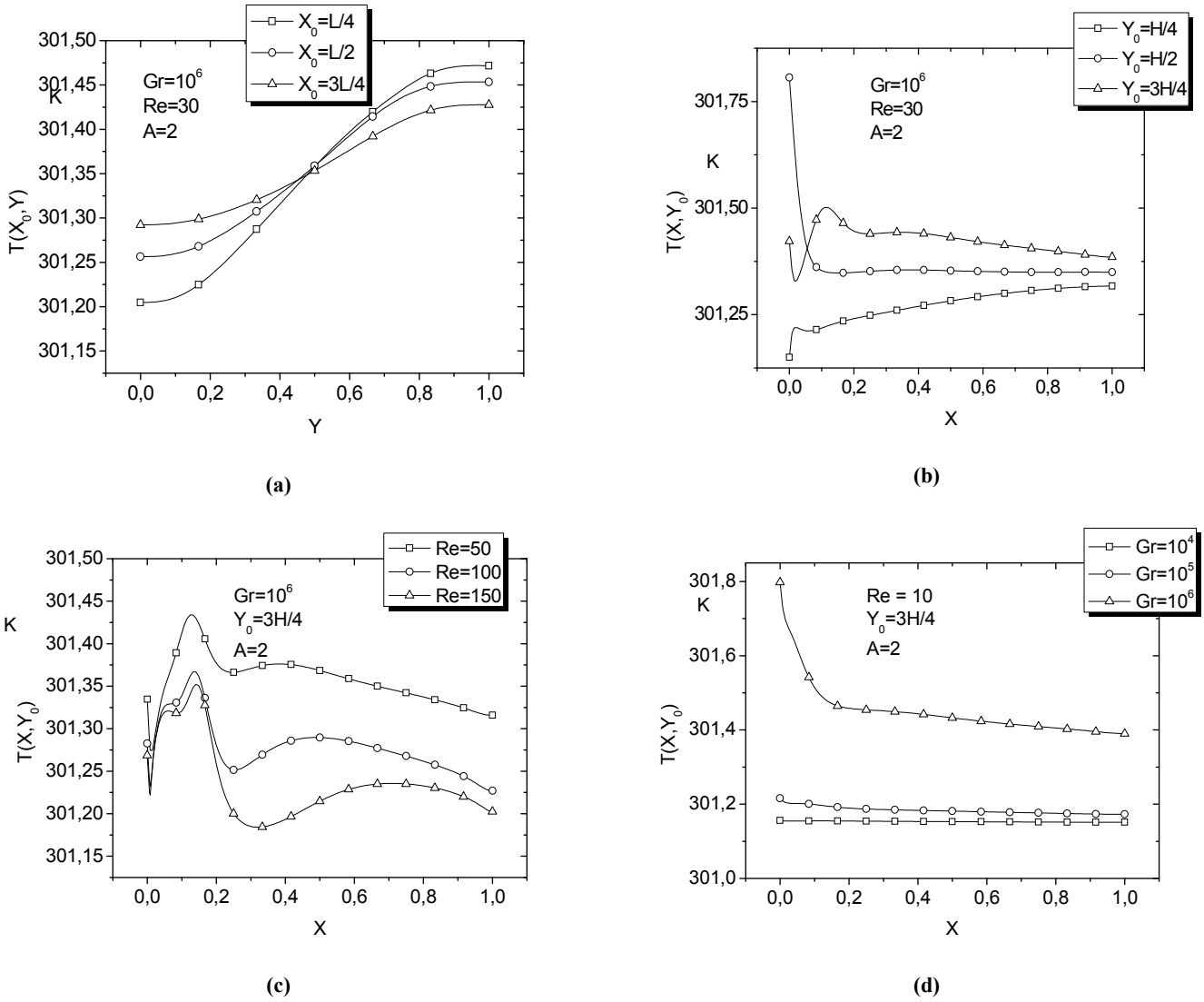

Fig.6. Variation of the temperature along the horizontal and vertical axis

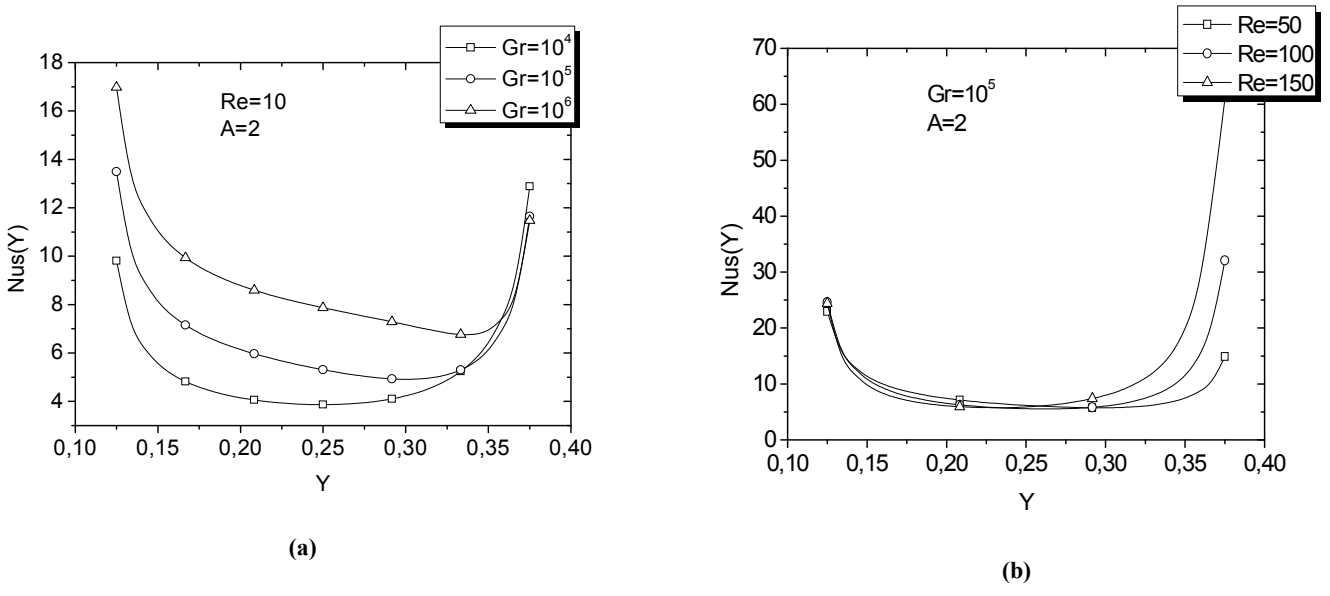

Fig.7. variation of local Nusselt number for various Grashof and Reynolds numbers

Configuration Case II: *Injections at the bottom and the top of the heated wall and exits from the bottom and the top of the cold wall where forced and natural convection aid each other*

Dynamic and thermal field

Effect of grashof number

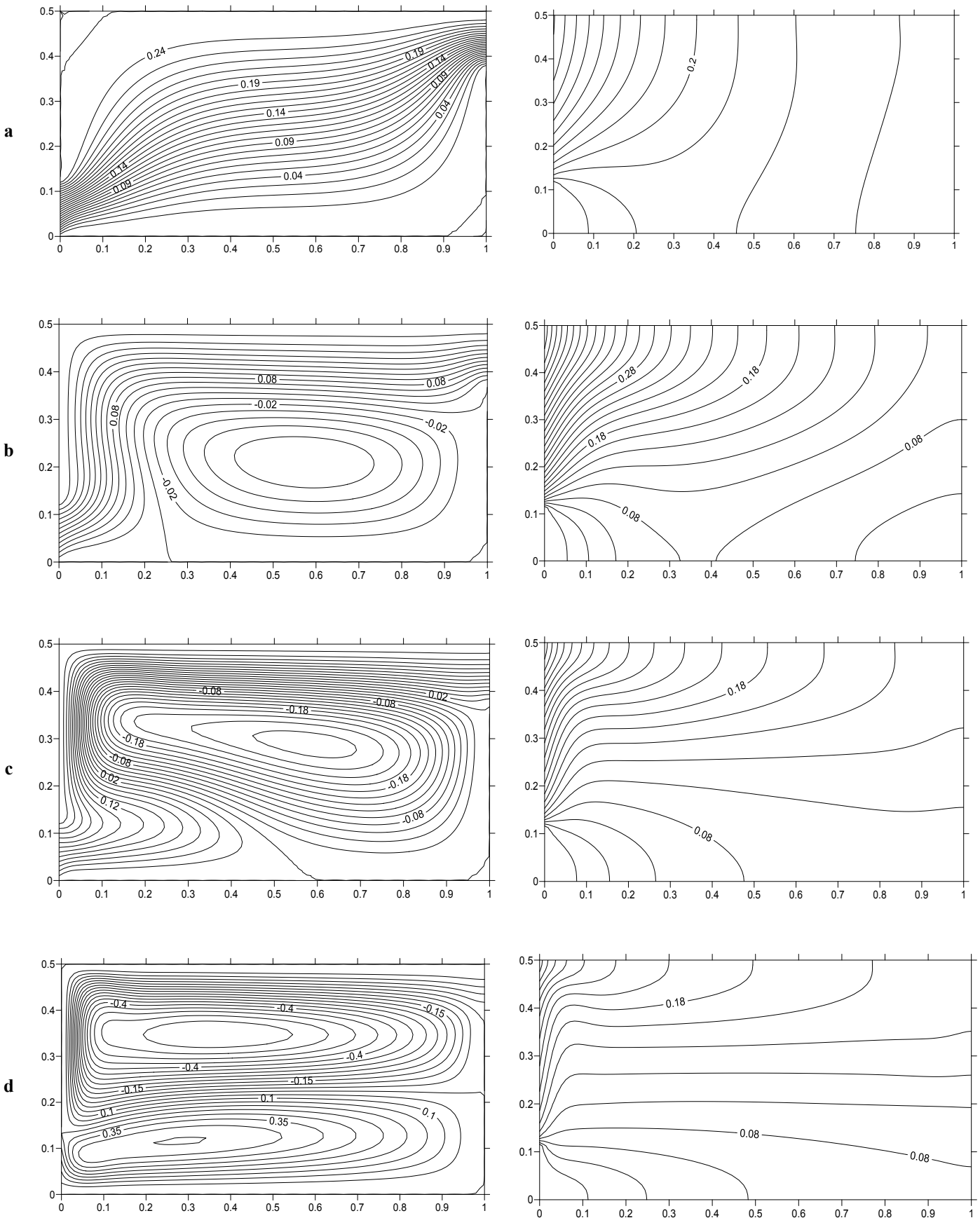

Fig .8. Streamlines and isotherms obtained for Re =10 and various values of Gr: (a) Gr= 0; (b) Gr= 10^4 ;(c) Gr=10^5; (d) Gr=10^6

For Gr = 0, (Re=10), Fig.8 (a) shows that the open lines of the external flow occupy almost the whole cavity from the lower entry opening to the upper exit. By increasing Gr up to 10^4, it can be seen from Fig.8 (b) that the open lines and the natural convective closed cells appear simultaneously in the cavity. A further increase in Gr gives rise to a variety of complex flow structures. Fig8.(c) shows that the open lines are constrained by the presence of the closed cells to describe an ``S'' trajectory. The corresponding isotherms show a good thermal stratification in the space over the lower opening, leading to zero horizontal temperature gradients. Thus, for Gr = 10^6, Fig. 8(d) shows that most of the open lines cross the cavity without being aspired by the left heated vertical wall and a closed shear cells is formed under the open lines. The corresponding isotherms are bifurcated and indicated the mixed convection manifestation in the vented building.

Effect of Reynolds number

The effect of the Reynolds number on fluid flow and temperature distribution is presented in Fig.9 (a-d) for a fixed Grashof number Gr = 10^6 and various Reynolds numbers. Fig. 9(a) shows, for Re = 30, the presence of a closed cells and located between the open lines of the forced flow. It is noteworthy that the cold forced flow descends the left heated vertical wall and imposes the rotation sense of the hot fluid in contact with the horizontal adiabatic surface.

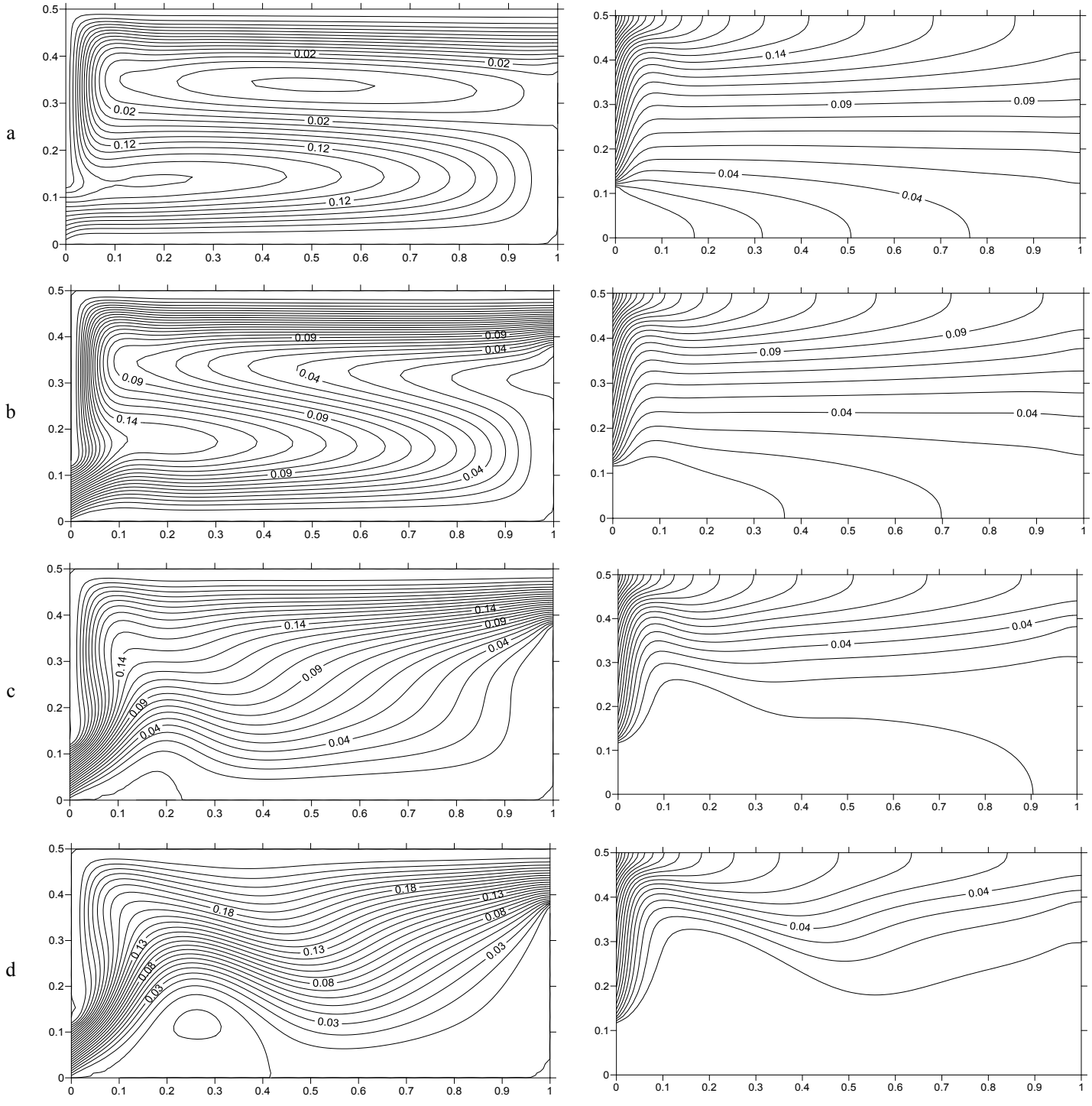

Fig.9. Streamlines and isotherms obtained for Gr=10^6 and various values of Re: (a) Re=30; (b) Re= 50; (c) Re=100; (d) Re=150

The velocity of the descending fresh air is reduced by the heating effect of the left vertical active wall favoring the formation of a small clockwise closed cells in the center of the cavity. The shape of the corresponding isotherms indicates that the temperature gradients are very weak in the horizontal direction if we except a thin region in the vicinity of the left heated vertical wall.

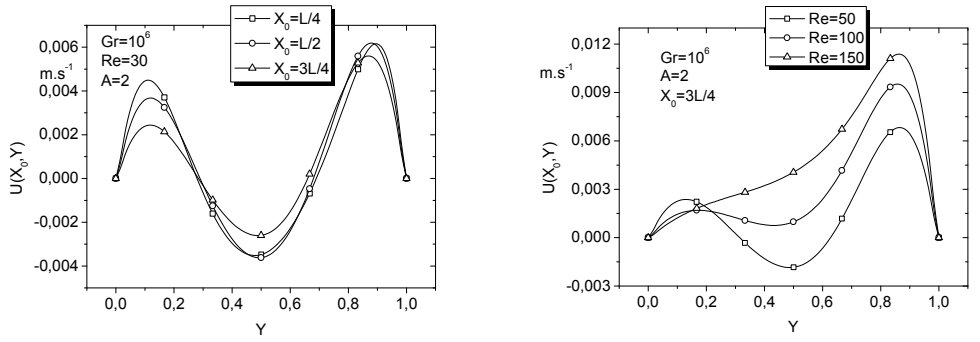

(a) **(b)**

Horizontal velocity component

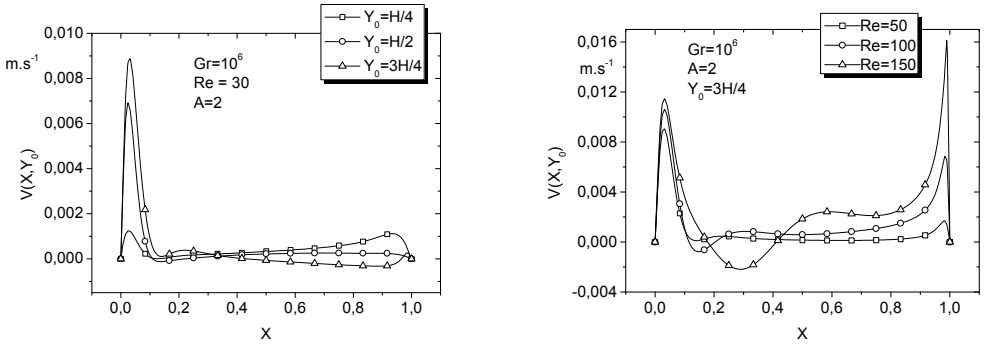

(c) **(d)**

Vertical velocity component

Fig.10. Variation of the flow velocity components in the cavity

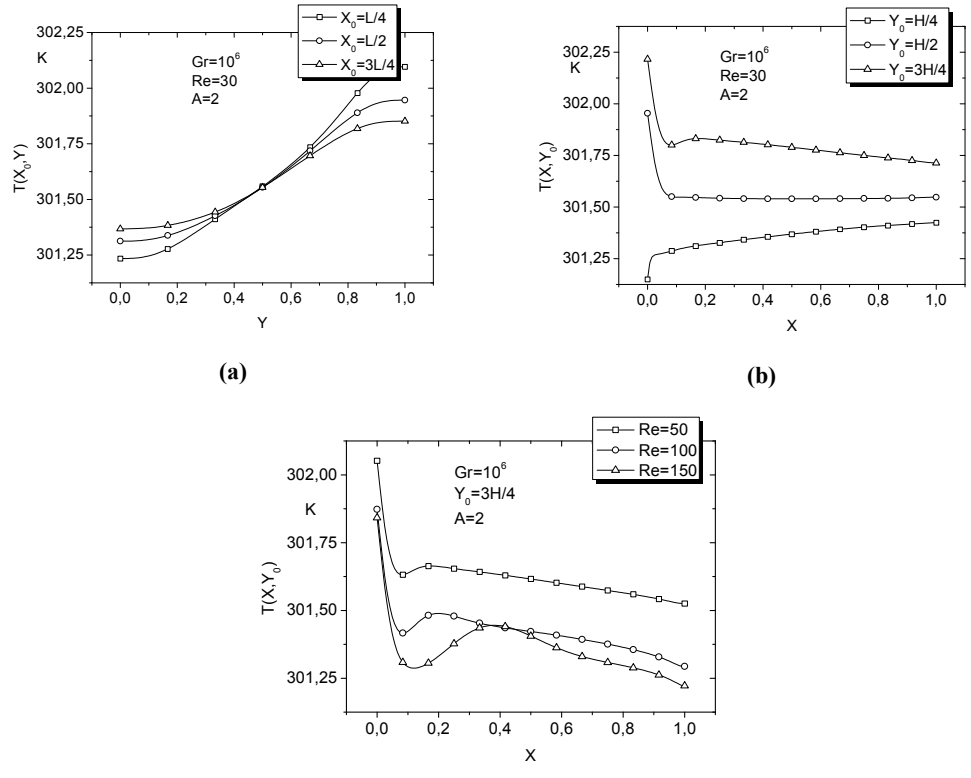

(a) **(b)**

(c)

Fig. 11. Variation of the temperature along the axis

A visible temperature stratification is observed near the left vertical active wall while all the remain part of the cavity is at the temperature of the cold jet. Qualitatively similar observations of ‘’S ‘’ trajectory for the open lines are shown in Fig. 9(b) for Re = 50. However, the increase of Re is not favorable to the natural convective cells which is at the limit of its disappearance.

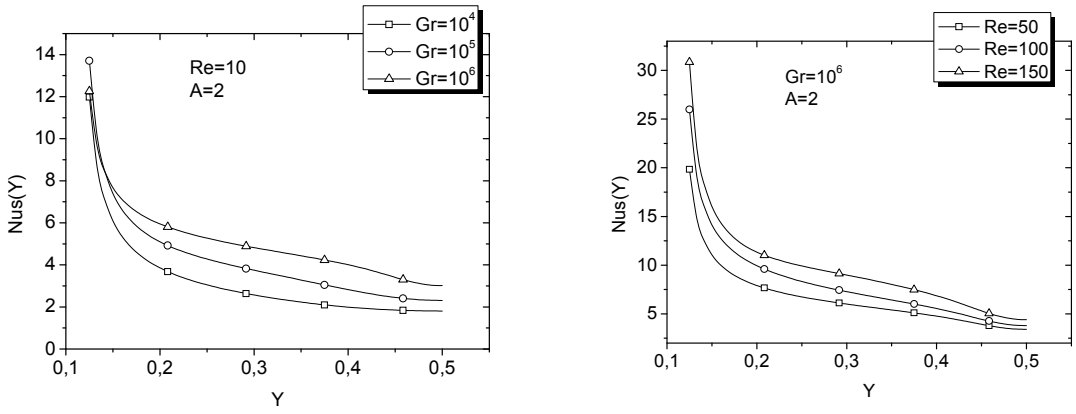

(a) (b)

Fig.12. Variation of local Nusselt number along the left heated wall for various Grashof and Reynolds numbers

In Fig. 9(c), only the open lines remain for Re =100. The temperature distribution shows the displacement of the isotherms front toward the lower part of the cavity. A further increase in the Reynolds number contributes to notably reducing the size of the closed cell situated between the open lines can be seen in Fig.9 (d) for Re = 150. This increase of Re favors now the formation of a natural convective closed cells in place of the one observed at lower values of the Reynolds number (Re =30). The effect of the forced convection increases significantly at higher values of Re, and the open lines cross the cavity diametrically through the openings without being affected by the left heated wall as shown in Fig.9(c, d) for Re = 100, and 150. Fig.10 (a-d) showed the variation of the flow velocity components along the horizontal and the vertical axis. The velocity components are increasing function of Reynolds number. The maximum values of the velocity components observed near the left heated and the right cold walls indicated that the heat and mass transfers are very important along the vertical walls. Hence the negative values indicated the recirculation zones in the vented cavity. The similar results are obtained by (Zerman S. *et al.,* 2005) in the numerical study of laminar mixed convection in the ventilated cavities. The fig.11(a, b) showed the variation of the isotherms along the horizontal and the vertical axis; then for the fixed Grashof and Reynolds numbers, the temperature is stratified in the two directions in the whole cavity. The heat transfer is important near the left heated wall. This situation indicated that the maximal value of the temperature is observed along the left heated wall, and the minimal value of the temperature is obtained on the floor of the cavity. One can observe in fig. 11 (c) that the temperature is a decreasing function of a Reynolds number. Since more increasing the Reynolds number, lower is the temperature in the cavity. Consequently, the thermal comfort is attained. Hence in fig.12(a, b), the local Nusselt number is a decreasing function along the heated wall for the fixed Grashof or Reynolds number. This variation of the local Nusselt number indicated that the heat transfer is important near the heated wall.

Configuration Case III: *Injections at the bottom of the heated and cold walls and exits from the top of the heated and cold walls where forced and natural convection aid each other*

Dynamic and thermal field

Effect of grashof number

In fig.13 (a), for Gr = 0, (Re=10), the open lines of the external flow occupy almost the whole cavity from the two entry openings. By increasing Gr up to 10^4, it can be seen from fig.13 (b) that the distorted open lines and the natural convective closed cells appear simultaneously in the cavity. A further increase in Gr gives rise to a rather formation of a clockwise cells near the floor of the cavity. Fig.13(c) shows that the open lines are constrained by the presence of the closed cells to describe an ``S'' trajectory. The corresponding isotherms show a good thermal stratification in the space over the lower opening, leading to zero horizontal temperature gradients. Thus, for Gr = 10^6, fig. 13(d) shows that most of the open lines cross the cavity without being aspired by the left heated vertical wall and a big closed shear cells is formed under the open lines. The corresponding isotherms are bifurcated and indicated the mixed convection manifestation in the vented building.

Effect of Reynolds number

The effect of the Reynolds number on fluid flow and temperature distribution is presented in Fig.14 (a-d) for a fixed Grashof number Gr = 10^6 and various Reynolds numbers. Fig. 14(a) shows, for Re = 30, the presence of a big closed cells located near the exit at the top of the heated wall and prevents the open lines of the forced flow to exit through the top openings. However, the increase of Re is not favorable to the natural convective cells which is at the limit of its disappearance, Fig.14 (b, c).

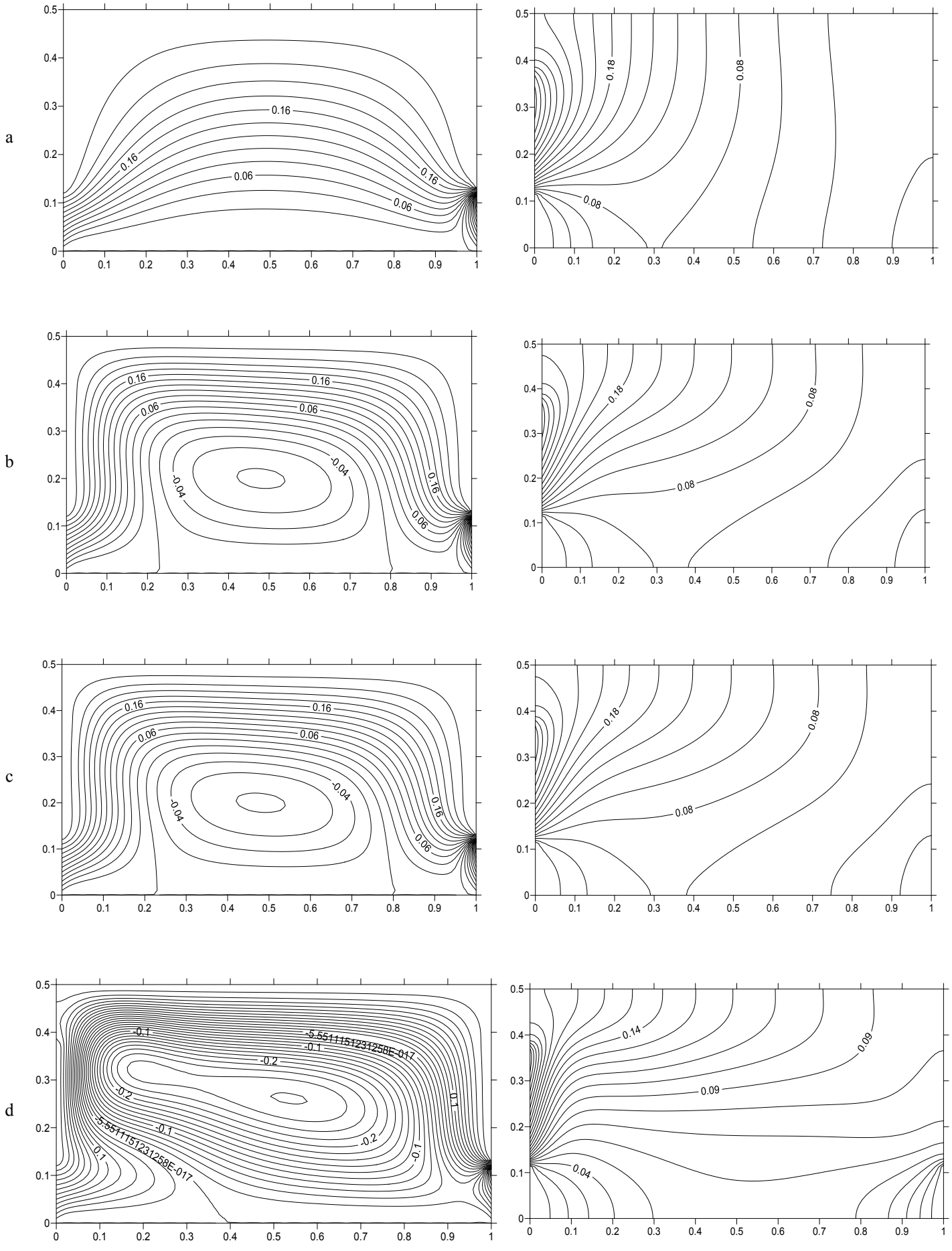

Fig.13. Streamline and isotherms obtained for Re=10 and various Grashof numbers: (a) Gr=0 ; (b) Gr=10^4; (c) Gr=10^5 ; (d) Gr=10^6

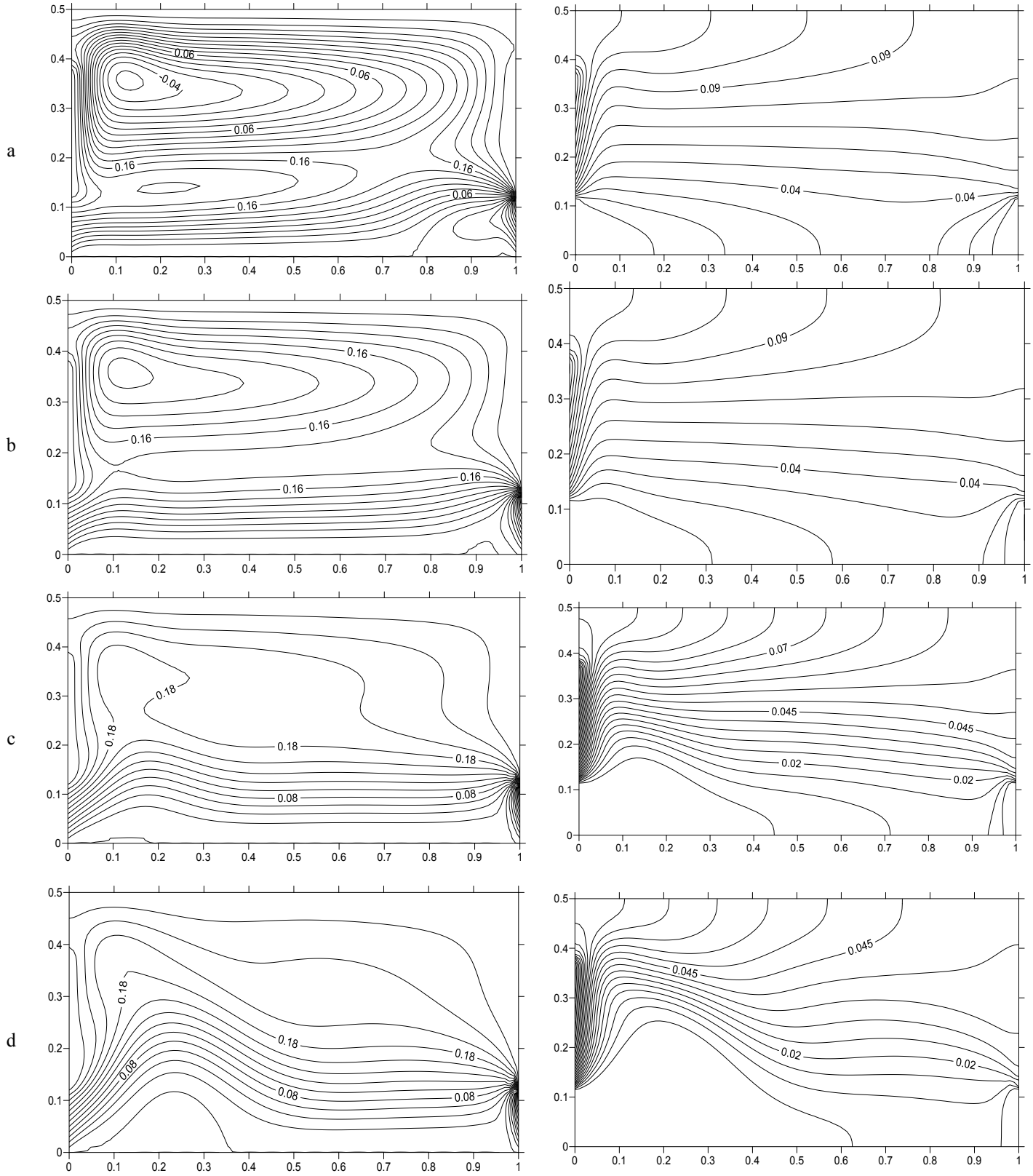

Fig.14. Streamline and isotherms obtained for Gr=10^6 an various Reynolds numbers: (a) Re=30; (b) Re=50; (C); Re=100; (d) Re=150

The temperature distribution shows the convective heat transfer is important in the hot zone near the heated wall. A further increase in the Reynolds number contributes to notably reducing the size of the closed cells situated between the open lines can be seen in Fig.14 (d) for Re = 150. This increase of Re favors now the formation of open lines in the whole cavity. The effect of the forced convection increases significantly at higher values of Re, and the open lines cross the cavity longitudinally through the openings without being affected by the left heated wall as shown in Fig.14(c, d) for Re = 100, and 150. The corresponding isotherms are tightened in the vicinity of the left heated vertical wall. The variation of the velocity components is exposed in Fig. 15(a-d). We found it useful to show this variation of the velocity components to clearly visualize the development of the given flow in form of the streamline by the Figs. (13,14).

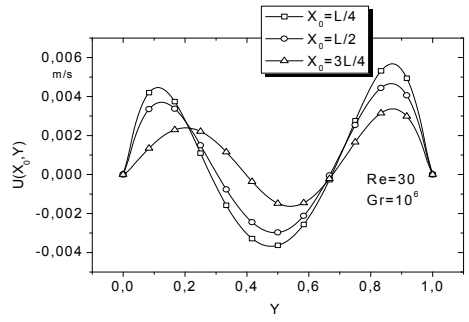

(a)

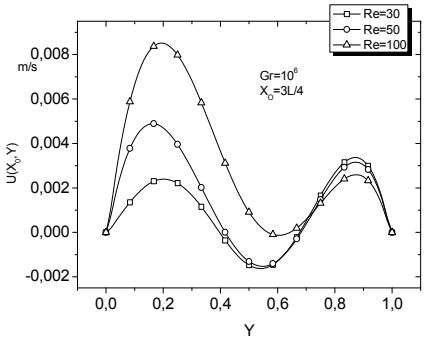

(b)

Horizontal component

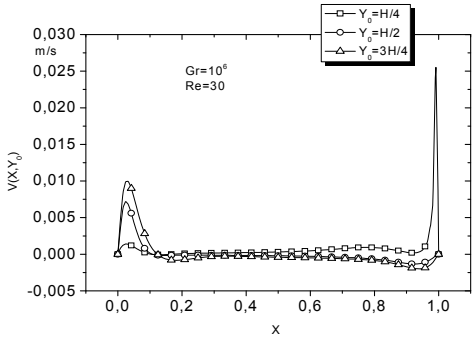

(c)

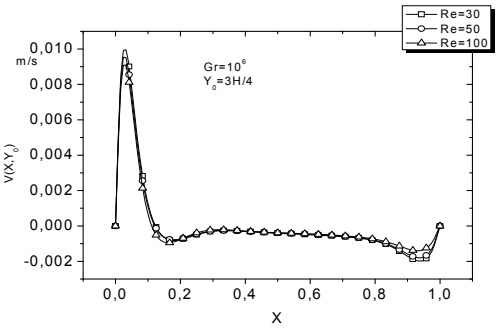

(d)

Vertical component

Fig.15. Variation of Flow velocity components along the axis

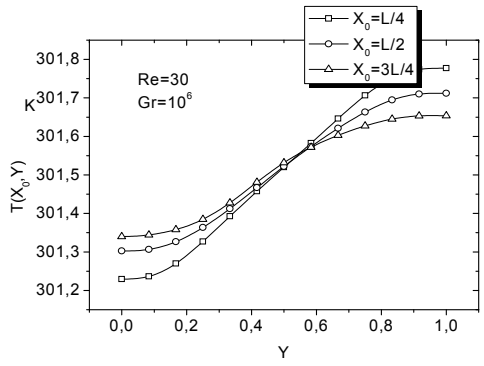

(a)

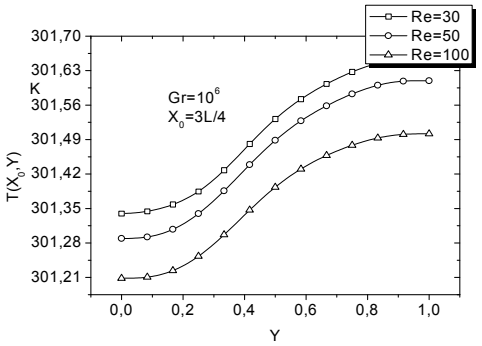

(b)

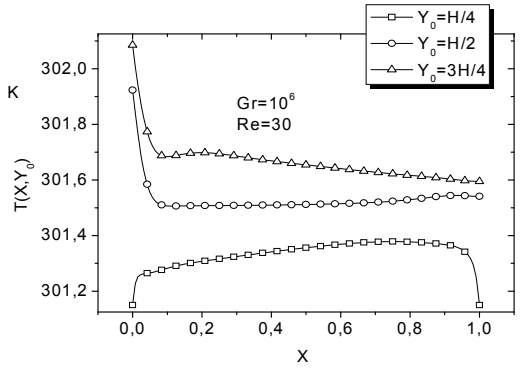

(c)

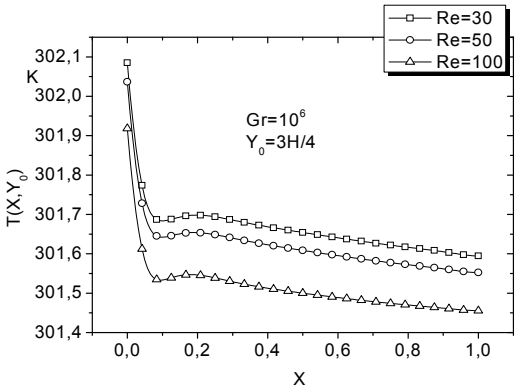

(d)

Fig.16. Variation of the temperature along the axis

Conclusion

A numerical simulation of laminar mixed convective venting in a building with different inlet or outlet openings location on the left heated and the right cold side walls has been conducted to identify the optimum placement of inlet and exit for the best cooling effectiveness. A total of three inlet/outlet placement configurations have been considered. The study encompasses a range of Reynolds number from 10 to 200 and a range of Grashof number from 0 to 10^6, representing dominating forced convection through mixed convection to dominating natural convection. The local Nusselt number at the heated wall, temperature in the cavity have been used to study the cooling effectiveness among different configurations. Results show that the fresh air injections at the bottom and the top of the heated walls and exits from the bottom and the top of the cold walls where forced and natural convection aid each other give the best cooling effectiveness and describe the ''S'' trajectory. Within the investigated parameters ranges, the following conclusions can be drawn.

- Significant gains in ventilation efficiency can be made by properly orienting and positioning of the inlet and outlet openings relative to each other and to the building.
- Inlets and outlets openings relative location give possibility to decrease conventional electrical energy consumption charge for air conditioning in the building.
- Inlets and outlets openings relative location provide passive venting and thermal comfort by natural convection in the building.

REFERENCES

Simoneau, J.P., Draoui, A. and Allard, F. 1989. ``Problèmes posés par la convection mixte dans la climatisation de l'habitat: première approche en régime laminaire", Revue Générale de Thermique, No. 325, pp. 31-39.

Safi, M.J. and Loc, T.P. 1994. ``Development of thermal stratification in a two-dimensional cavity: a numerical study", *Int. J. Heat Mass Transfer,* Vol. 37 No. 14, pp. 2017-24.

Yao, L.S. 1983. ``Free and forced convection in the entry region of a heated vertical channel", *Int.J. Heat Mass Transfer,* Vol. 26 No. 1, pp. 65-72.

Humphrey, J.A.C. and To, W.M. 1986. ``Numerical simulation of buoyant turbulent flow ± I. Free convection along a heated, vertical, flat plate. II. Free and mixed convection in a heated cavity", *Int. J. Heat Mass Transfer,* Vol. 29 No. 4, pp. 573-610

Hsu, T.H., Hsu, P.T. and How, S.P. 1997. `Mixed convection in a partially divided rectangular enclosure", Numerical Heat Transfer, Part A, Vol. 31, pp. 655-83.

Raji, A. and Hasnaoui, M. 1998a. ``Mixed convection heat transfer in a rectangular cavity ventilated and heated from the side", Numerical Heat Transfer, Part A, No. 33, pp. 533-48.

Jones W.P., B.E. Launder, 1972. The prediction of laminarization with a two-equation model of turbulence, *Int. J. Heat Mass Transfer,* 15, PP 301–314.

Terai T. Indoor Thermal Convection, Architectural Institution of Japan, Japan, 1959, p. 63, (in Japanese).

Nomura T., M. Kaizuka, 1973. in: Numerical Calculation Method of Air Distribution, Architectural Institution of Japan, Japan, 1972, p. 4,(1973) in Japanese.

Tsuchiya T. 1973. Application of Meteorological Numerical Calculation Method to Indoor Air flows, Architectural Institution of Japan, Japan, 1973 (in Japanese).

Yamazaki H., Y. Urano, M. Nashida, T. Watanabe, 1976. Comparison of Numerical Calculation and Visualization Experiments of Two-dimensional Flows, Architectural Institution of Japan, Japan, 1976, p. 240, in Japanese

Nomura T., Y. Matsuo, M. Kaizuka, Y. Sakamoto, K. Endo, 1975Numerical Study of Room Air Distribution, Parts I and II, Architectural Institution of Japan, Japan , pp. 231–232, in (Japanese.).

Catton, I. 1979. Natural convection in enclosures, in: Proceedings of 6th Int. Heat Transfer Conference, Toronto Vol. 6, pp. 13–43.

Ostrach S. (1972), Natural convection in enclosure, in: J.P. Hartnell, T.F. Irvine _Eds.., Advances in Heat Transfer Vol. 8 Academic Press,New York, 1972.

Lage J.L., A. Bejan, R. Anderson, 1991. Efficiency of transient contaminant removal from a slot ventilated enclosure, Int. J. Heat Mass Transfer 34 (10). (1991), PP. 2603–2615.

Lage J.L., A. Bejan, R. Anderson, 1992. Removal of contaminant generated by a discrete source in a slot ventilated enclosure, Int. J. Heat Mass Transfer 35 (5). (1992), PP. 1169–1180.

Kato S., S. Murakami, S. Kondo, 1994. Numerical simulation of two dimensional room airflow with and without buoyancy by means of ASM, ASHRAE Trans. 100 1994,PP. 238–255, Part 1.

Murakami S., S. Kato, R. Ooka, 1993. Numerical study on horizontal non-isothermal jet in room with DSM and $k-\varepsilon$ model, in: Proceedings of International Symposium on CFD, Sendai, Japan,1993.

Hsu T.H., P.T. Hsu, S.P. How, 1997. Mixed convection in a partially divided rectangular enclosure, Numer. Heat Transfer, Part A 31 (1997), PP. 655–683.

Lee S.C., C.Y. Cheng, C.K. Chen, 1997. Finite element solutions of laminar and turbulent flows with forced and mixed convection in an air-cooled room, Numer. Heat Transfer, Part A 31, PP. 529–550.

Shaw H.J. 1993. Laminar mixed convection heat transfer in three-dimensional horizontal channel with a heated bottom, Numer. Heat Transfer, Part A 23 (1993), PP. 445–461.

Williams P.T., A.J. Baker, 1994. CFD characterization of natural convection in a two-cell enclosure with a door, ASHRAE Trans. 100 (1994),PP. 685–696, Part 2.

Baek C.I., K.S. Lee, W.S. Kim, 1997. Study of combined heat transfer in a three-dimensional enclosure with a protruding heat source, Numer. Heat Transfer, Part A 32 (1997), PP. 733–747

Woods L.C. 1954. A note of numerical solution of fourth differential equations, Aero. Q. 5, 176-l 84.

Raji A., M. Hasnaoui, 2000. Mixed convection heat transfer in ventilated cavities with opposing and assisting flows. http://www.emerald-library.com.PP. 556 - 572.

Zermane S., Boudebous S., Boulkroune N. 2005. Etude numérique de la convection mixte laminaire dans des cavités ventilées,Sciences and Technologie B- N° 23, Juin 2005, PP. 34-44.

****